Molecular Dynamics Simulations of Ground and Transition States for the Hydride Transfer from Formate to NAD⁺ in the Active Site of Formate Dehydrogenase

Rhonda A. Torres, Birgit Schiøtt,[†] and Thomas C. Bruice*

Contribution from the Department of Chemistry, University of California, Santa Barbara, California 93106

Received April 20, 1999

Abstract: Formate dehydrogenase (FDH) from *Pseudomonas* sp. 101 is a homodimeric enzyme that catalyzes oxidation of formate and the concomitant reduction of NAD⁺ to produce NADH and CO₂. The dynamic motions and distances between functional groups in the active site of the formate dehydrogenase including the NAD⁺ cofactor and substrate have been investigated by molecular dynamics (MD) simulations, incorporating the substrate in one subunit (E·S) and the transition state in the other subunit (E·TS). Experimental kinetic isotope effects and calculated isotope effects are in excellent agreement, thus, the transition state in the enzymatic reaction is expected to closely resemble the structure determined by ab initio calculations. The simulation shows that the formate is held in place by persistent electrostatic interactions consisting of a bifurcated hydrogen bond between one formate oxygen and the guanido hydrogens of Arg284, and single hydrogen bonds from the other formate oxygen to a side chain amide proton of Asn146 and the backbone amide proton of Ile122. The conserved residues Arg284, Asn146, and Ile122 serve as pivots about which the C−H of formate swings to and from the C4N of NAD⁺. The C4N of NAD⁺ and the formate hydrogen are in position to react (near attack conformations, NACs) approximately 1.5% of the simulation time. An additional effect of the hydrogen bonding of the formate oxygens to Arg284, Asn146, and Ile122 is to prevent nucleophilic attack of the carboxylate on NAD⁺ to form an ester, which is the reaction favored in the gas phase. His332 plays a role in both the binding of formate and the generation of the near attack conformations. Further insight into the roles of other conserved amino acids (Pro97, Phe98, Asp308, and Ser334) at the catalytic site is provided. Comparisons of the electrostatic interactions at the active site of the enzyme with substrate and transition state show changes in hydrogen bonding due to charge differences; however, these changes are not consistent with the hypothesis of preferential stabilization of the transition state over the ground state.

Introduction

Formate dehydrogenase (FDH, EC 1.2.1.2) is a member of a large class of NAD⁺-dependent dehydrogenases. FDH catalyzes the NAD⁺-dependent oxidation of formate to CO₂ (eq **1**). It is

$$NAD^+ + HCO_2^- \rightarrow NADH + CO_2 \qquad (1)$$

a dimer with two identical subunits, each of which possesses an NAD⁺ and substrate binding site.[1,2] The two active sites are known to function independently of one another.[3] The reaction involves the cleavage of a carbon−hydrogen bond in the substrate and the formation of a carbon−hydrogen bond in the product (NADH) without proton release or abstraction. From kinetic measurements, it is known that this bi-substrate reaction follows an ordered mechanism in which NAD⁺ binds first followed by formate.[4−7] In addition, it has been shown that hydride transfer is the rate-limiting step in the oxidation of

formate to CO₂.[4,6] Catalysis occurs on the A-side of the NAD⁺ pyridine ring,[8] and the carboxamide group is in the *trans* conformation,[2,3] such that the carboxamide oxygen of NAD⁺ is pointing in the direction of the C4N of the pyridine ring (Scheme 1).

Much attention has been paid to the conformation of the nicotinamide ring in the transition state of the formate dehydrogenase reaction.[4−7,9−14] Accurate ¹⁵N isotope effect measurements[7] and recent gas phase ab initio calculations[13] have shown that the nitrogen center is almost planar during the transition state of the reaction (Scheme 1b). This is also in accord with

* To whom correspondence should be addressed. E-mail: tcbruice@ bioorganic.ucsb.edu.

† Current address: Aarhus Katedralskole, Skolegyde 1-3, 8000 Århus C, Denmark.

(1) Lamzin, V. S.; Aleshin, A. E.; Strokopytov, B. V.; Yukhnevich, M. G.; Popov, V. O.; Harutyunyan, E. H.; Wilson, K. S. *Eur. J. Biochem.* **1992**, *206*, 441.

(2) Lamzin, V. S.; Dauter, Z.; Popov, V. O.; Harutyunyan, E. H.; Wilson, K. S. *J. Mol. Biol.* **1994**, *236*, 759.

(3) Popov, V. O.; Lamzin, V. S. *Biochem. J.* **1994**, *301*, 625.

(4) Blanchard, J. S.; Cleland, W. W. *Biochemistry* **1980**, *19*, 3543.

(5) Cook, P. F.; Oppenheimer, N. J.; Cleland, W. W. *Biochemistry* **1981**, *20*, 1817.

(6) Hermes, J. D.; Morrical, S. W.; O'Leary, M. H.; Cleland, W. W. *Biochemistry* **1984**, *23*, 5479.

(7) Rotberg, N. S.; Cleland, W. W. *Biochemistry* **1991**, *30*, 4068.

(8) Rossman, M. G.; Liljas, A.; Bränden, C.-I.; Banaszak, L. J. In *The Enzymes*; Boyer, P. D., Ed.; Academic Press: New York, 1975; Vol. 11A, p 61.

(9) Almarsson, Ö.; Karaman, R.; Bruice, T. C. *J. Am. Chem. Soc.* **1992**, *114*, 8702.

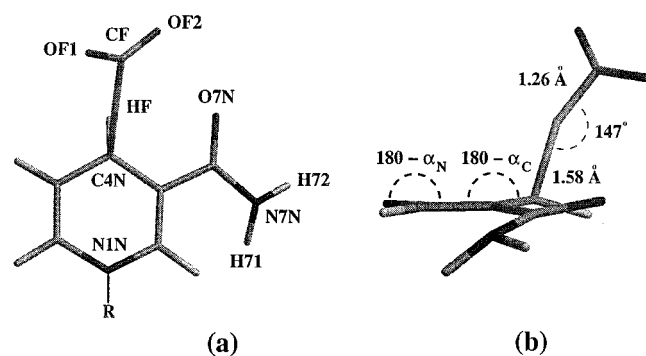(10) Almarsson, Ö.; Bruice, T. C. *J. Am. Chem. Soc.* **1993**, *115*, 2125.

(11) Tapia, O.; Andrés, J.; Cardenas, R. *Chem. Phys. Lett.* **1992**, *189*, 395.

(12) Wu, Y. D.; Lai, D. K. W.; Houk, K. N. *J. Am. Chem. Soc.* **1995**, *117*, 4100.
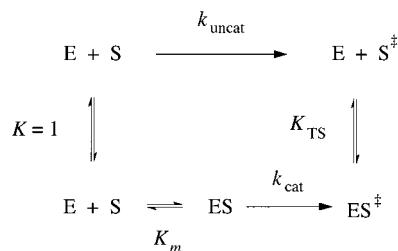
(13) Schiøtt, B.; Zheng, Y.-J.; Bruice, T. C. *J. Am. Chem. Soc.* **1998**, *120*, 7192.

(14) Hutchins, J. E. C.; Binder, D. A.; Kreevoy, M. M. *Tetrahedron* **1986**, *42*, 993.

Scheme 1

(a)　　　　　　　　　　　(b)

Scheme 2

previous theoretical studies.[12,15−24] The calculated primary k_H/k_D isotope effect for hydride transfer (2.91)[13] is in good agreement with those observed experimentally when 10-methylacridinium $(2.1−3.1)$[14] or the NAD+ of FDH (3.14)[7] are formate oxidants. As made obvious by Alhambra and co-workers,[25] differences in k_H/k_D isotope effects determined experimentally and by quantum mechanical calculations may result from changes which are unaccounted for in the calculations, e.g. tunneling. This is, however, not an issue for secondary isotope effects with heavy atoms such as ^{15}N. The ab initio calculated secondary ^{15}N isotope effect for the nicotinamide ring nitrogen is in excellent agreement with that determined for the enzyme, 1.0042 vs 1.004 ± 0.001, respectively. Combined, the k_H/k_D and the ^{14}N/^{15}N isotope effects support the proposal that the transition state structure for the oxidation of formate in the gas phase is quite similar to that in FDH and the pyridine nitrogen remains near planar in the transition state.

The "thermodynamic cycle" of Scheme 2 compares the transformation of a reactant (S) to its transition state in solution (S‡) and to its transition state (E·S‡) when S is enzyme bound (E·S). The dissociation constant (K_{TS}) for E·S‡ can be calculated from the experimentally determined constants $\{K_{TS} = (k_{uncat}/(k_{cat}/K_m)\}$.[26] The assumption that K_{TS} is generally significantly smaller than the constant for dissociation of E·S is in accord with the generally accepted proposal[27,28] that enzymatic reactions

(15) Andrés, J.; Moliner, V.; Safont, V. S.; Domingo, L. F.; Picher, M. T. *J. Org. Chem.* **1996**, *61*, 7777.
(16) Andrés, J.; Moliner, V.; Safont, V. S.; Domingo, L. R.; Picher, M. T.; Krechl, J. *Bioorg. Chem.* **1996**, *24*, 10.
(17) Andrés, J.; Moliner, V.; Safont, V. S. *J. Phys. Org. Chem.* **1996**, *9*, 498.
(18) Buck, H. M. *Recl. Trav. Chim. Pays-Bas* **1996**, *115*, 329.
(19) Cummins, P. L.; Gready, J. E. *J. Comput. Chem.* **1991**, *11*, 791.
(20) Cunningham, M. A.; Ho, L. L.; Nguyen, D. T.; Gillilan, R. E.; Bash, P. A. *Biochemistry* **1997**, *36*, 4800.
(21) Mestres, J.; Duran, M.; Bertrán, J. *Bioorg. Chem.* **1996**, *24*, 69.
(22) Wu, Y.-D.; Houk, K. N. *J. Am. Chem. Soc.* **1987**, *109*, 2226.
(23) Wu, Y. D.; Houk, K. N. *J. Am. Chem. Soc.* **1991**, *113*, 2353.
(24) Wu, Y. D.; Houk, K. N. *J. Org. Chem.* **1993**, *58*, 2043.
(25) Alhambra, C.; Gao, J.; Corchado, J. C.; Villà, J.; Truhlar, D. G. *J. Am. Chem. Soc.* **1999**, *121*, 2253.
(26) Kurz, J. L. *J. Am. Chem. Soc.* **1963**, *85*, 987.
(27) Wolfenden, R. *Acc. Chem. Res.* **1972**, *5*, 10.

are driven by preferential binding of S‡ over S. A challenge to this generally accepted proposal has been presented by Cannon and Benkovic,[29] who have established the relationships of eqs **2** and **3**.

$$\log k_{uncat} \simeq -1.0 \log K_{TS} + A \qquad \text{with } r = 0.96 \qquad (2)$$

$$\log k_{cat} \simeq -0.2 \log K_{TS} + B \qquad \text{with } r = 0.5 \qquad (3)$$

Examination of eq 2 shows an excellent linear free energy relationship between the rate constant of the uncatalyzed reaction (k_{uncat}) and K_{TS}. From eq 3, there is no relationship between the rate constant for the enzymatic reaction and K_{TS}. Whatever the explanation for eq 2, it is obvious that K_{TS}, as calculated from Scheme 2, has nothing to do with the value of the rate constant for the enzymatic reaction. A means of observing the interactions of the enzyme with both the S and the TS would be of great value as a tool to assist in understanding enzyme catalysis. This is particularly so for a number of enzymes where preferable binding of TS over S is supported by studies with transition state analogues.[30] As a first step in this direction we have examined by molecular dynamic simulation (MD) the E·S and E·TS complexes of FDH.

The X-ray crystal structure of the holoenzyme (hFDH) from *Pseudomonas* sp. 101, with NAD+ cofactor and azide ion inhibitor, has been reported[2] to a resolution of 2.05 Å (Brookhaven Protein Data Bank, refcode: 2nad). In their experimental paper, Lamzin et al.[2] suggested, based on the binding of azide, that formate could adopt two possible orientations in the catalytic site of FDH. In orientation 1, the formate is bound between Arg284 and Asn146 such that a salt bridge forms between a formate oxygen and one hydrogen of the guanidinium group of Arg284, while the second formate oxygen is hydrogen bonded to Asn146. In orientation 2, the formate is bound between His332 and Asn146, but no charge neutralization by histidine is possible as the presence of Gln313 prevents His332 from becoming protonated. The authors noted that based on the crystal structure, neither orientation was optimal for catalysis, but orientation 1 was more likely. Here, we report the preferred binding orientation of formate and the conformational changes that occur in both the E·S and E·TS complexes during the 2 ns MD simulation. For our purposes, a formate molecule replaces the azide inhibitor in one of the two subunits. In the second subunit, the calculated TS structure for the hydride transfer reaction[13] replaces the azide. This study provides additional insight into the roles of conserved amino acids at the catalytic site.

Methods and Computational Details

All molecular dynamics simulations were performed using the Amber 5.0 suite of programs[31] with the Cornell et al. force field[32] and using RESP charges.[33] Neither NAD+ nor formate are found in the Amber

(28) Schowen, R. L. In *Transition States of Biochemical Processes*; Gandour, R. D., Schowen, R. L., Eds.; Plenum Press: New York, 1978; p 78.
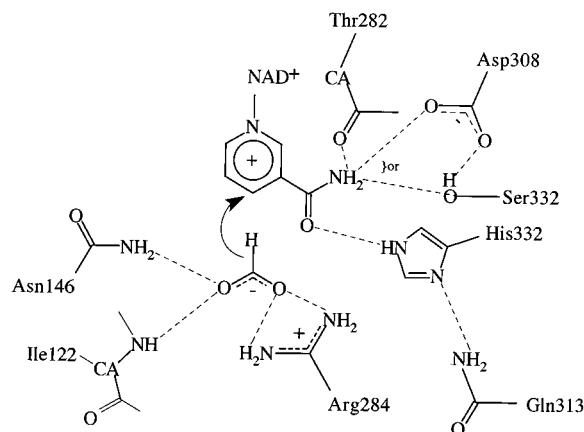(29) Cannon, W. R.; Benkovic, S. J. *J. Biol. Chem.* **1998**, *273*, 26257.
(30) Schramm, V. L. *Annu. Rev. Biochem.* **1998**, *67*, 693.
(31) Case, D. A.; Pearlman, D. A.; Caldwell, J. W.; Cheatham, T. E. I.; Ross, W. S.; Simmerling, C. L.; Darden, T. A.; Merz, K. M.; Stanton, R. V.; Vincent, J. J.; Crowley, M.; Ferguson, D. M.; Radmer, R. J.; Seibel, G. L.; Singh, U. C.; Weiner, P. K.; Kollman, P. A. *Amber 5.0*; San Francisco, 1997.
(32) Cornell, W. D.; Cieplak, P.; Bayly, C. I.; Gould, I. R.; Merz, K. J.; Ferguson, D. M.; Spellmeyer, D. C.; Fox, T.; Caldwell, J. W.; Kollman, P. A. *J. Am. Chem. Soc.* **1995**, *117*, 5179.
(33) Cornell, W. D.; Cieplak, P.; Bayly, C. I.; Kollman, P. A. *J. Am. Chem. Soc.* **1993**, *115*, 9620.

Scheme 3

Figure 1. Root-mean-square deviation for the secondary structure elements in the E·S (black) and the E·TS (gray) complexes, referenced to the starting structure.

database. Very recently, NAD$^+$ has been made available with the Cornell et al. force field with RESP charges by Ryde et al. and we used these numbers directly.[34] RESP charges for formate and TS were estimated using the structure from our preceding ab initio study of the reduction of formate by a nicotinamide and *N*-alkyl nicotinamides at the HF/6-31+G(d,p) level of theory.[13] Merz–Kollman[35,36] electrostatic potential points were calculated in Gaussian94 at the HF/6-31G(d) level of theory.[37] We used 10 layers with 17 points per unit area in the ESP calculation for formate and for the TS model as recommended by Sigfridsson and Ryde.[38] The computed partial charges, atom types and atomic labels used for formate, NAD$^+$, and TS are listed in the Supporting Information. Force constants for these three residues were estimated by comparing to similar structures. For NAD$^+$ and the TS, dihedral parameters for the rotation of the carboxamide group were taken from Vanhommerig et al.[39] To maintain the structure of the TS throughout the MD simulation, we assigned high force constants for the bond lengths and bond angles of the TS structure essentially making it a rigid body. All added force constants are listed in the Supporting Information.

The starting structure was prepared by modifying the crystal structure of the ternary complex of FDH with bound NAD$^+$ and azide inhibitor, as determined by Lamzin et al. (Brookhaven Protein Database: 2nad) at 2.05 Å resolution.[2] Each subunit consists of 393 amino acid residues. In subunit A, formate was docked into the active site with the carbon positioned over the central azide nitrogen and the hydrogen to be transferred directed toward the C4N position of NAD$^+$. The azide ion was deleted from the coordinate file. In subunit B, the azide and the nicotinamide ring were removed and the transition state structure was anchored through the N1N to the protein X-ray structure. The geometry of the nicotinamide–formate TS moiety was taken from the ab initio optimized TS for hydride transfer from formate to *N*-alkyl nicotinamides.[13] All crystallographic waters were included in the model, and the system was additionally solvated by an 8.0 Å layer of waters. All water molecules were treated as TIP3P[40] residues. A second layer of waters were added to the system from 7 to 10 Å. The system contained 36334 atoms (a total of 8866 residues) including 8089 molecules of water. Energy minimization (10000 steps of steepest descents followed

by 10000 steps of conjugate gradient) was done to alleviate any unfavorable contacts in the two active sites and between the two layers of water. Restraints on the outer shell waters were applied during the conjugate gradient minimization, which was necessary to avoid the loss of water molecules during the dynamics simulation. The resulting energy minimized complex represents the starting structure for the molecular dynamics simulations. The standard nomenclature for atoms in the amino acid residues was used.

Molecular dynamics was initiated by letting the system heat up linearly over 20 ps from 0 to 300 K, and it was kept at 300 K throughout the simulation by coupling to a heat bath. The step size was chosen to be 0.002 ps and the nonbonded interactions were cut off at 10.0 Å, with the list updated every 25 steps. The SHAKE[41] algorithm was used to constrain all bonds involving hydrogen atoms. Coordinates were saved every 0.2 ps for analysis. After the initial 20 ps of heat up, harmonic constraints were applied to the water molecules in the outer shell to keep them from departing during the simulation. Average distance and angle values were calculated after 160 ps. Root-mean-square (RMS) deviations from initial structures were calculated using the α carbons in the protein backbone. The positional fluctuations of the atoms were obtained from the available *B*-factors[2] utilizing the equation $\langle \Delta r^2 \rangle^{1/2} = (3B/8\pi^2)^{1/2}$.[42] The per residue RMS fluctuation was calculated after 160 ps. The kinetically essential near attack conformation (NAC)[43–45] is defined as having a (formate)H1–(NAD$^+$)C4N distance of ≤ 3.0 Å and a (formate)C1–(formate)H1–(NAD$^+$)C4N angle between 132° and 180°. The attack distance was chosen based on the van der Waals radii of neutral molecules containing hydrogen and carbon while the attack angle was chosen based on previously calculated[13] transition state structures in the gas phase and in acetonitrile.

Results and Discussion

In our MD simulations, the formate was docked in the active site of FDH from *Pseudomonas* sp. 101[2] with the hydrogen directed toward the C4N of NAD$^+$ to form the E·S complex. No constraints were applied to maintain this interaction, thus the formate anion was free to adopt the energetically most favored position. Scheme 3 depicts the binding environment adopted by formate in the E·S subunit during the MD simulation. Many features are similar to those proposed by Lamzin and

(34) Ryde, U. *Protein Sci.* Submitted for publication.

(35) Besler, B. H.; Merz, K. M. J.; Kollman, P. A. *J. Comput. Chem.* **1990**, *11*, 431.
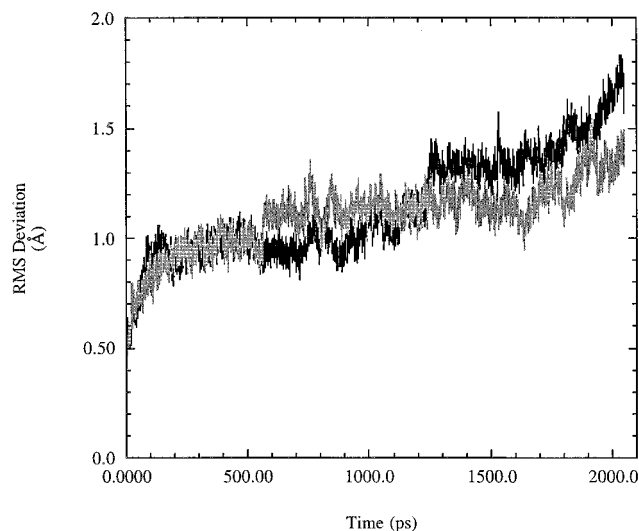
(36) Singh, U. C.; Kollman, P. A. *J. Comput. Chem.* **1984**, *5*, 129.

(37) Frisch, M. J.; Trucks, G. W.; Schlegel, H. B.; Gill, P. M. W.; Johnson, B. G.; Robb, M. A.; Cheeseman, J. R.; Al-Laham, M. A.; Zakrzewski, V. G.; Ortiz, J. V.; Foresman, J. B.; Cioslowski, J.; Stefanov, B. B.; Nanayakkara, A.; Challacombe, M.; Peng, C. Y.; Ayala, P. Y.; Chen, W.; Wong, M. W.; Andres, J. L.; Replogle, E. S.; Gomperts, R.; Martin, R. L.; Fox, D. L.; Binkley, J. S.; Defrees, D. J.; Baker, J.; Stewart, J. J. P.; Head-Gordon, M.; Gonzalez, C.; Pople, J. A. *Gaussian94 B.2*; Gaussian, Inc., Pittsburgh, PA, 1995.

(38) Sigfridsson, E.; Ryde, U. *J. Comput. Chem.* **1998**, *19*, 377.

(39) Vanhommerig, S. A. M.; Sluyterman, L. A.Æ.; Meijer, E. M. *Biochim. Biophys. Acta-Protein Struct. Mol. Enzymol.* **1996**, *1295*, 125.

(40) Jorgensen, W. L.; Chandrasekhar, J.; Madura, J. D. *J. Chem. Phys.* **1983**, *79*, 926.

(41) van Gunsteren, W. F.; Berendsen, H. J. C. *Mol. Phys.* **1977**, *34*, 1311.

(42) McCammon, J. A.; Harvey, S. C. *Dynamics of Proteins and Nucleic Acids*; Cambridge University Press: Cambridge, 1987.

(43) Lightstone, F. C.; Bruice, T. C. *J. Am. Chem. Soc.* **1994**, *116*, 10789.

(44) Lightstone, F. C.; Bruice, T. C. *J. Am. Chem. Soc.* **1996**, *118*, 2595.

(45) Lightstone, F. C.; Bruice, T. C. *J. Am. Chem. Soc.* **1997**, *119*, 9103.
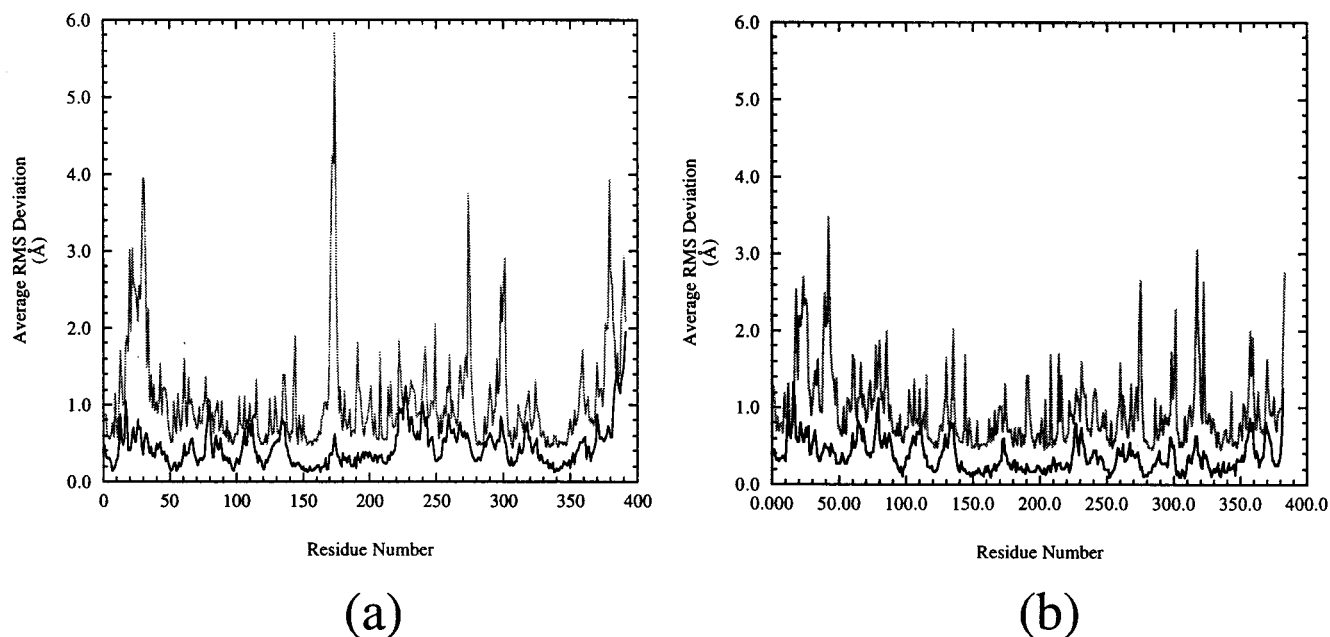
Figure 2. Plot of the average root-mean-square deviations for each α carbon in the E·S complex (a) and the E·TS (b) complex.

co-workers[2] for binding orientation 1; however, some notable differences exist. Figure 1 shows the RMS deviation of snapshots from the trajectory from the crystal structure. The RMS deviation peaked at 1.8 Å from the crystal structure and the structural changes were very small over time, suggesting the simulation equilibrated. The per residue RMS fluctuation comparison to the provided *B*-factors is shown in Figure 2a for the E·S complex and Figure 2b for the E·TS complex. A large per residue RMS deviation was observed involving the loop formed by residues 171−174. This loop connects two small α helices and is located on the surface of the protein. This large RMS deviation is due to a slow repositioning of this surface loop, presumably due to the charged side chains interacting with the solvent. In a similar manner, the other large RMS per residue fluctuations (above 3.0 Å) also appear to be due to charged amino acid side chains in random loops on the surface of the protein.

We first examine the enzyme−substrate (E·S) complex to determine the probability of forming near attack conformations (NACs). The results obtained from examination of the MD simulations of the E·S complex are then compared to the simulation of the E·TS complex.

Interactions in the Enzyme−Substrate Complex. Upon binding of the substrate in the active site, the carboxylate group of formate forms a salt bridge with the guanidinium group of Arg284 and hydrogen bonds with the amide group of Asn146 as well as with the backbone hydrogen of Ile122. The interaction of formate with Arg284, Asn146, and Ile122 restricts the orientations that formate can adopt in the active site such that it does not tumble freely. The negative charge on the formate oxygens is matched by the positive charge on the guanido group of Arg284. The bifurcated-type hydrogen bonds formed between guanidinium protons (HH22 and HH12) and the O2 formate oxygen are stable throughout the simulation with average distances of 1.99 ± 0.23 and 1.86 ± 0.13 Å, respectively. The importance of Arg284 to substrate binding and catalysis has been established by chemical modification and mutagenesis experiments.[3,46] It was suggested that ancillary functions of

Arg284 include stabilizing the hydride being transferred and charge perturbation in the NAD$^+$ ring.[3] However, this is not supported by the MD simulations. The O1 of formate forms hydrogen bonds with the backbone −NH of Ile122 and an amide side chain hydrogen (HD21) of Asn146. These interactions are also stable throughout the simulation with average distances of 1.99 ± 0.24 and 1.88 ± 0.17 Å, respectively.

The electrostatically stabilizing interactions formed between the formate oxygens and Arg284, Asn146, and Ile122 result in the creation of a pivot about which the formate hydrogen oscillates with respect to the C4N of NAD$^+$. Figure 3 depicts this oscillating motion. The side chain of Ile122 (as well as Pro97 and Phe98, *vide infra*) prevents 360° rotation of the formate hydrogen about this pivot axis. The allowed motions of formate over the simulation time can be expressed in terms of the distance and the angle of approach of the formate hydrogen to the C4N of NAD$^+$. Conformations that approach the distance and angle requirements for hydride transfer, determined from our previous ab initio calculations,[13] represent near hydride transfer or near attack conformations (NACs). Various conformations during the simulation time are shown in Figure 4. We have assigned NACs as structures with attack angles (C4N···H···CO$_2^-$) between 132° and 180° and a distance of approach of ≤3.0 Å. NACs are observed during 1.5% of the sampled simulation time.

Amino acids Val150 and Ile202 are located on the distal face (B-side) of the nicotinamide ring relative to the substrate. These two amino acids are conserved for all known sequences of FDH.[3] This B-side shielding of the NAD$^+$ accounts for the hydride transfer reaction occurring only to the A-side of the NAD$^+$ ring. Due to the bulky side chains of Val150 and Ile202, slight anisotropic puckering of the ring toward the substrate, α_C (Scheme 1a), occurs with an average value of 3.6 ± 5.17°. The average α_N was calculated to be 0.88 ± 3.76°, which suggests that the pyridine nitrogen in the NAD$^+$ ring remains essentially planar in the E·S complex.

The amide oxygen of Ile122 is at an average distance of 4.06 ± 1.32 Å (minimum distance = 1.43 Å) from the 2′-OH hydrogen of the NAD$^+$ ribose. This interaction places the 2′-oxygen of NAD$^+$ directly above the N1N of the pyridine ring

(46) Egorov, A. M.; Tishkov, V. I.; Popov, V. O.; Berezin, I. V. *Biochim. Biophys. Acta* **1981**, *659*, 141.
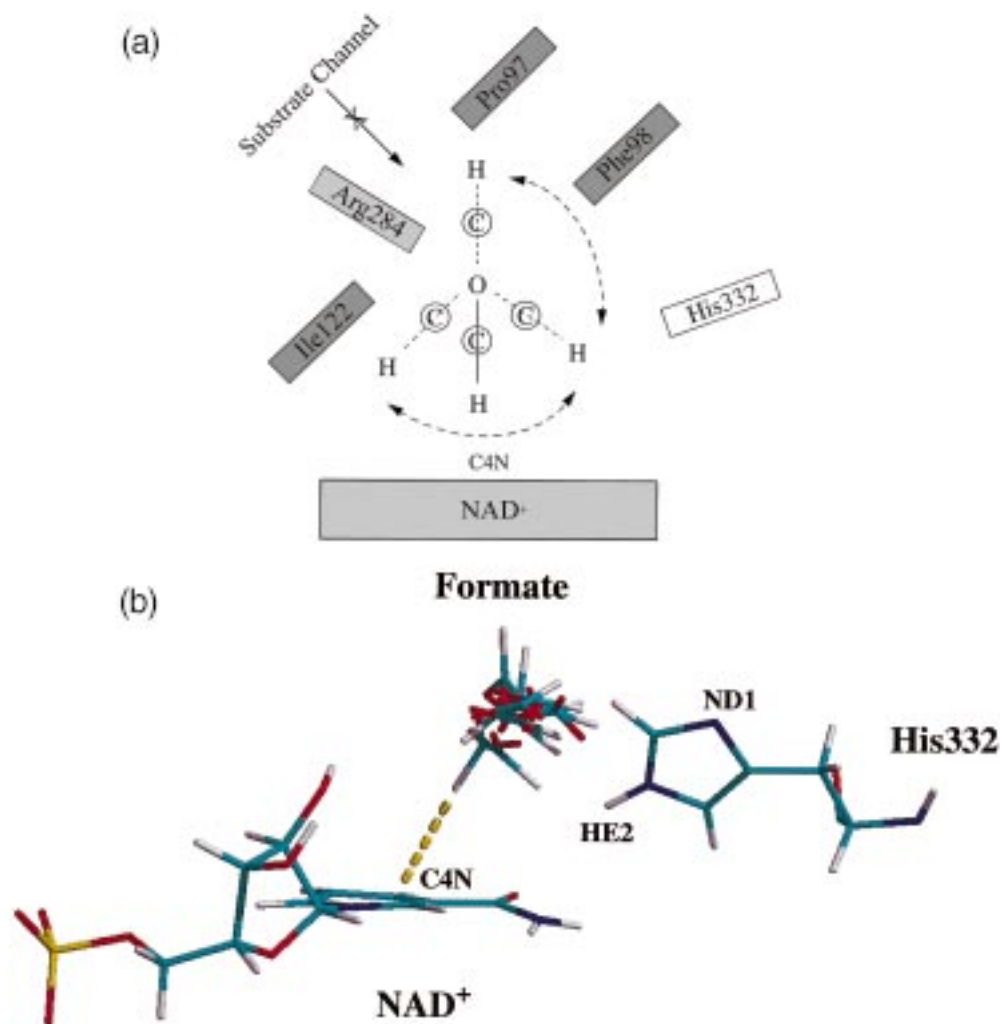
Figure 3. (a) Schematic representation of the C–H moiety motions of formate within the active site of FDH. (b) Snapshots from production dynamics depicting the range of motion that the hydride to be transferred from formate to the nicotinamide ring of the cofactor undergoes during the simulation. The dashed yellow line represents a near hydride transfer conformation, NAC, from the simulation with a hydride transfer angle of 174° and hydride transfer distance of 2.78 Å. For clarity, only the formate and the catalytically relevant portions of the NAD^+ and His332 associated with the NAC structure are shown.

with an average distance of 3.42 ± 0.22 Å. Figure 5 depicts the distance between N1N and 2′O over the production dynamics for the E·S (Figure 5a) and E·TS (Figure 5b) complexes. It is interesting to note that the closest contacts between these two atoms in the E·S complex correspond to a substantial number of NAC structures. The side chain of Ile122 is also oriented partially above the pyridine ring. These interactions between Ile122 and the NAD^+ are complementary to a planar nitrogen in the pyridine ring.

The amino acids Thr282, Asp308, Ser334, and His332 form persistent hydrogen bonds to the carboxamide group of NAD^+ (Scheme 3). These interactions position the NAD^+ with the carboxamide moiety in a *trans* conformation. The *trans* carboxamide is the only conformation found in enzymatic systems and it has been proposed to provide assistance to hydride transfer.[3,19,47] The backbone oxygen of Thr282 participates in a hydrogen bond with the H71 atom of the carboxamide arm of NAD^+ with an average distance of 1.87 ± 0.12 Å. There is also a hydrogen bond that alternately involves either the side chain hydroxyl oxygen (OG) of Ser334 or a side chain carboxyl oxygen (OD1) of Asp308 with the remaining amide proton of the carboxamide (H72). Figure 6 represents histograms of these

alternating hydrogen bonds between Ser334 (Figure 6a) and Asp308 (Figure 6b) with H72 of NAD^+. The average H72···OG distance is 2.69 ± 0.40 Å (min. = 1.61 Å) while the average H72···OD1 distance is 3.78 ± 0.58 Å (min. = 1.78 Å). The other carboxylate oxygen of Asp308 (OD2) participates in a persistent hydrogen bond with the HG of Ser334 with an average distance of 2.19 ± 0.53 Å (Scheme 3). The side chain of His332 also helps to maintain the carboxamide group in a *trans* conformation with a hydrogen bond between the ϵ proton (HE2) of the histidine and the O7N of the NAD^+ carboxamide (average distance 2.25 ± 0.35 Å).

Several interesting features were noted upon examination of the motions of His332. In addition to the persistent hydrogen bond formed between the HE2 of His332 and the O7N of NAD^+, hydrogen bonds were formed, at times, between the HE2 of His332 and the formate hydrogen or a formate oxygen. It was observed that NAC formation is associated with the formate hydrogen and the His332 HE2 approaching one another to an average distance of 3.02 ± 0.71 Å (with a minimum distance of 1.46 Å). An example of this interaction is shown in Figure 7. This hydrogen–hydrogen interaction comes about from the differences in the partial negative charge on the formate hydrogen (−0.1945 au, Scheme 4 and Supporting Information)

(47) Wu, Y. D.; Houk, K. N. *J. Am. Chem. Soc.* **1987**, *109*, 2226.
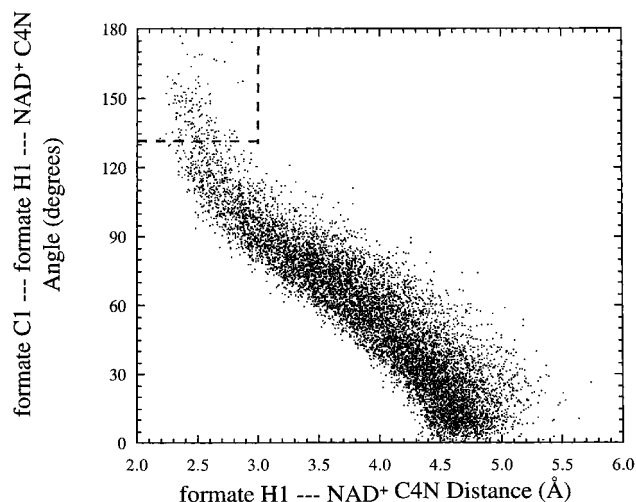
Figure 4. Plot of the hydride transfer angle vs hydride transfer distance of the structures produced in the molecular dynamics simulation. The boxed portion formed by the dotted lines represents those conformations located that are NAC structures. The average hydride transfer (attack) angle is 54° (maximum = 177°) and the average hydride transfer (attack) distance is 3.95 Å (minimum = 2.19 Å).

and the partial positive charge on HE2 of His332 (0.3324 au).[31] The question arises as to the possible role of the ϵ proton of the histidine imidazole orienting the hydrogen to be transferred as hydride toward the C4N of NAD^+. Experiments have shown that His332 is important to formate binding.[48] The hydrogen bond between His332 HE2 and O7N of NAD^+ is somewhat lengthened when HE2 of His332 interacts with the formate hydrogen, but remains a stabilizing influence as evidenced by the relatively short average distance when His332 HE2 interacts with the NAD^+ carboxamide (*vide supra*). It was also noticed that close contacts developed between the O1 of formate and the HE2 of His332 (Scheme 3), the average distance between these two atoms being 2.84 ± 0.40 Å with the closest distances observed in NAC structures (Figure 8).

Residues His332 and Gln313 are conserved in all known sequences of FDH enzymes.[3] The δ nitrogen (ND1) of His332

participates in a persistent hydrogen bond with an amide side chain proton (HE21) of Gln313 (Scheme 3). The average distance between the ND1 of His332 and the HE21 of Gln313 is 2.11 ± 0.25 Å. It appears that the primary role of the glutamine is to position the histidine imidazole such that it can assist in formate binding. Further support of this conclusion has been reported in mutagenesis studies where the glutamine was mutated to glutamate with retention of activity.[48]

A plot of the distance separating formate H1 and His332 HE2 vs formate H1 and NAD^+ C4N distance (Figure 9) shows that a portion of conformational space is not readily accessible to these atoms. The MD simulation reveals that the side chain of Phe98 inhibits the unfettered oscillation of formate (Figure 10) about the pivot formed between formate and Arg284, Asn146, and Ile122 (*vide supra*, Figure 1a). Residues Pro97 and Phe98 are conserved in all known sequences of FDH.[3] These residues are proposed to form a "wall" at the end of the substrate binding channel, which serves to exclude water from the catalytic site.[2,3] Compressive motions of the Pro97 (Figure 11a) and Phe98 side chains toward the formate oxygen (O2) were observed during the simulation. The average distance of Pro97 HG3 to formate O2 is 4.69 ± 0.59 Å, with the shortest distances corresponding to NAC structures. Thus, the motions of the Pro97 (and Phe98) toward the formate oxygen assist in NAC formation and also restrict greater motion of the formate hydrogen away from the C4N of NAD^+. Favorable hydrophobic stacking interactions between Pro97, Phe98, and His332 were also observed and represent a portion of the pre-structuring forces in the creation of the active site.

**Interactions in the Enzyme−Transition State Complex.** It should be possible to determine the differential roles of the conserved amino acid residues by comparisons of the structures of the active site in E·S and E·TS complexes. The interaction of the enzyme functional groups with the formate and NAD^+ in the E·S complex (Scheme 3) are much the same as their interactions with the transition state in the E·TS complex. Changes in the bond lengths of some electrostatic interactions

(a)

(b)
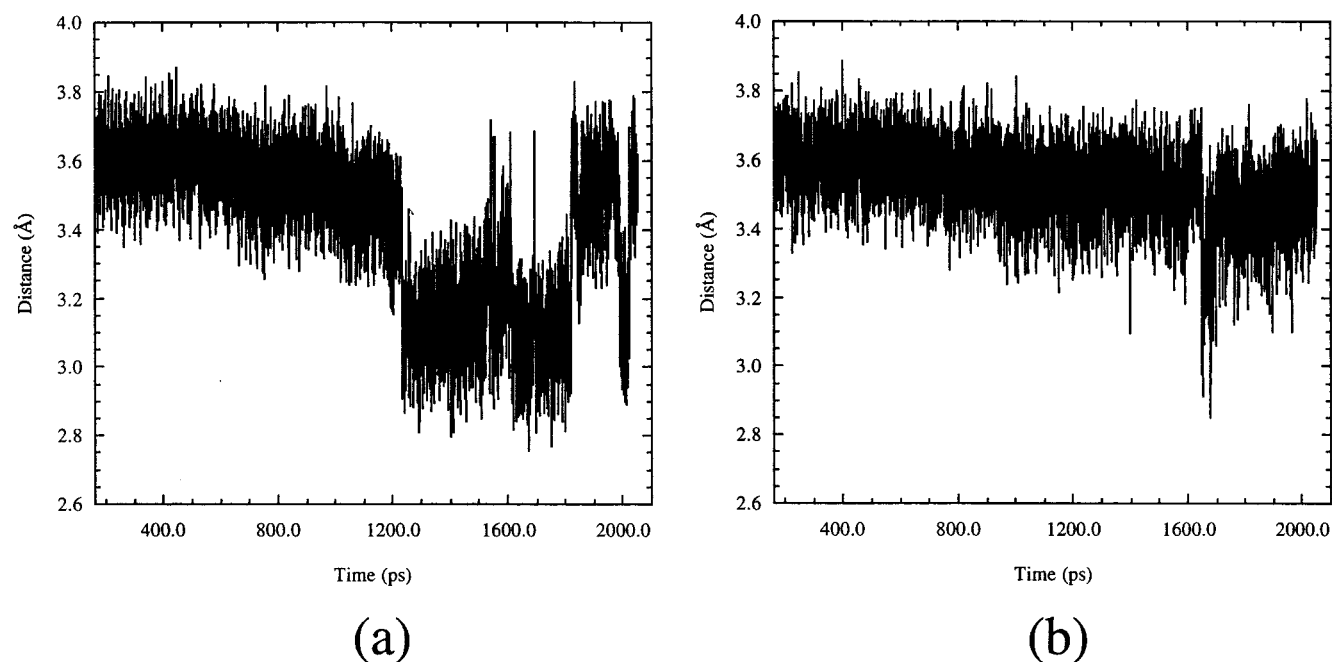
Figure 5. Plots of the distance between the ribose oxygen and the N1N of NAD^+ for both the E·S (a) and E·TS (b) complexes. Note the close contacts between these two atoms between 1.2 and 1.8 ns for the E·S complex. This region corresponds to the production of many NAC structures.
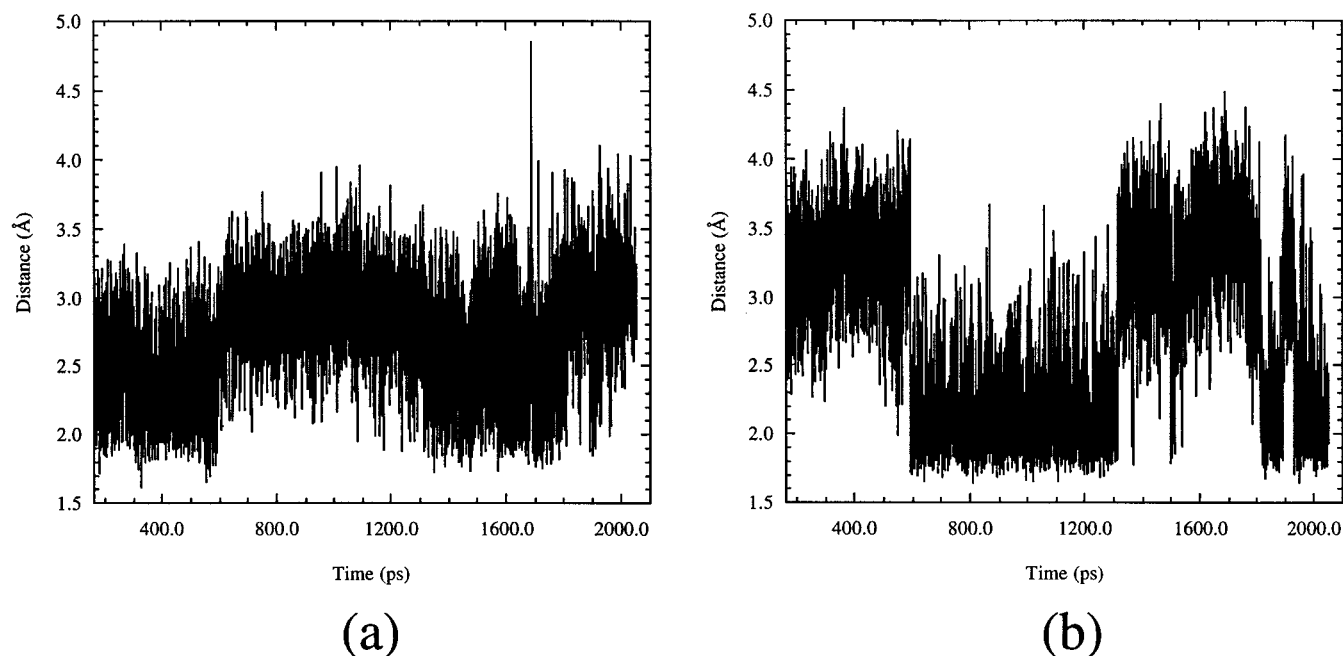
Figure 6. Histogram of the distances between H72 of the carboxamide arm of NAD$^+$ and the Ser334 OG (a) and Asp308 OD1 (b), respectively. These two hydrogen bonding interactions with the H72 amino proton appear to work in concert to maintain the *trans* conformation of the carboxamide arm. The regions corresponding to short distances between H72 and the OG of Ser334 relate to the formation of many NAC structures.
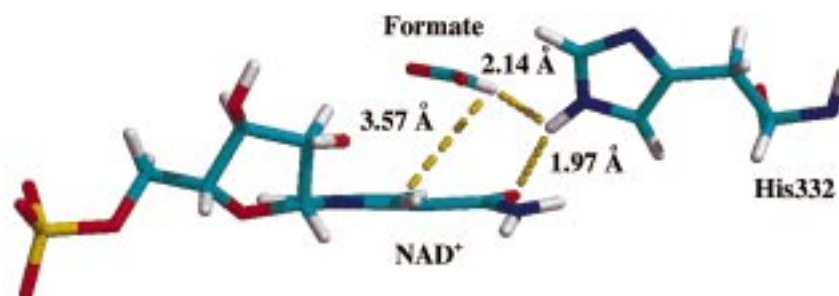

Figure 7. Snapshot showing the close approach of the hydrogen of formate and HE2 of His332 prior to the formation of a NAC structure.

Scheme 4
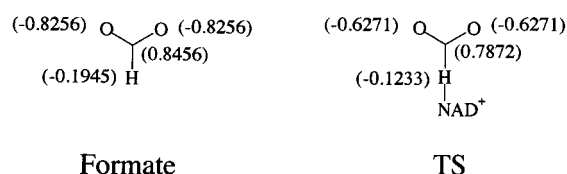
reflect changes in the electron density of enzyme bound ground state and transition state.

In the E·TS complex, the average distances for the bifurcated hydrogen bond between OF2 and Arg284 guanido group hydrogens (HH12 and HH22) are 2.02 ± 0.18 and 2.32 ± 0.29 Å, respectively. These average distances are 0.16–0.34 Å longer than those found in the same bifurcated hydrogen bond in the E·S complex. The average hydrogen bond distance between OF2 (formate oxygen) of the TS and HE2 (His332) is 3.19 ± 0.45 Å, which can be compared to the same hydrogen bond in the E·S complex (2.84 ± 0.40 Å). The increases in the bond lengths are expected on the basis that the negative charge on the carboxylate is attenuated in the TS. Thus, the electrostatic bonding of Arg284 and His332 to formate, which accommodates the negative charge and positions the ground state, is at least
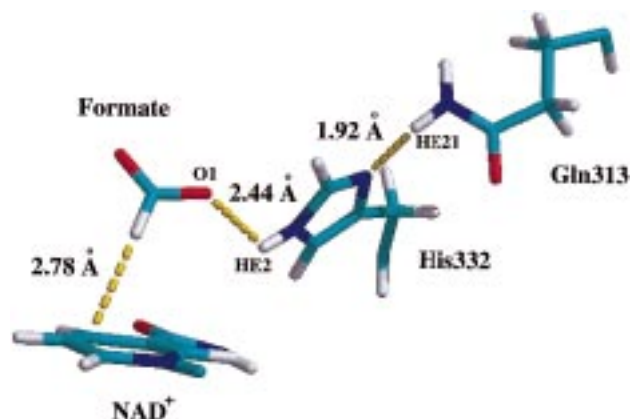

Figure 8. Snapshot of a NAC structure displaying the stabilizing effect produced when HE2 of His332 interacts with a formate oxygen in the E·S complex. Note the tight hydrogen bond that exists between His332 and Gln313 which persists throughout the simulation.

as important as that observed in the transition state. Residues Asn146 and Ile122 form hydrogen bonds with the OF1 carboxylate oxygen of the TS with average distances of 1.94 ± 0.14 and 2.05 ± 0.19 Å, respectively. These distances are roughly the same as in the E·S complex.

In the E·TS complex, as in the E·S complex, Thr282 and Ser334 form persistent hydrogen bonds to the carboxamide

(48) Tishkov, V. I.; Matorin, A. D.; Rojkova, A. M.; Fedorchuk, V. V.; Savitsky, P. A.; Dementieva, L. A.; Lamzin, V. S.; Mezentzev, A. V.; Popov, V. O. *FEBS Lett.* **1996**, *390*, 104.
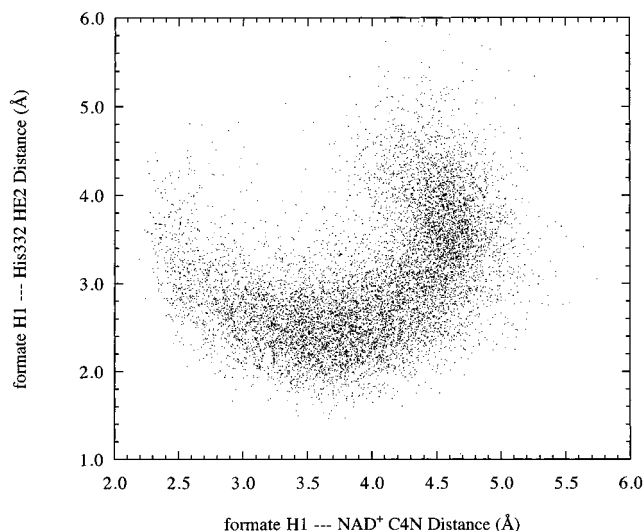
Figure 9. Plot of the formate hydrogen to His332 HE2 distance vs the attack distance (formate hydrogen to NAD$^+$ C4N distance). From this figure, it can be seen that a region of conformational space is not readily available to these atoms and suggests a potential barrier to the hydride transfer reaction.

group of NAD$^+$. The average distance between the backbone oxygen of Thr282 and the amide proton H71 of NAD$^+$ is almost identical to that found in the E·S complex (1.88 ± 0.12 Å). The OG of Ser334 participates in a persistent hydrogen bond with the other amide proton (H72) of the NAD$^+$ (average distance, 2.55 ± 0.35 Å). The OD1 atom of Asp308 also interacts with H72 of NAD$^+$ with an average distance of 3.58 ± 0.56 Å. In this complex, Ser334 hydrogen bonds to H72 but Asp308 does not. This is in contrast to the situation observed in the E·S complex where both Ser334 and Asp308 alternate in hydrogen bonding interactions with H72 of NAD$^+$ (compare Figures 6 and 12). In the E·TS complex, the average distance between the carboxyl oxygen of Asp308 (OD1) and the hydroxyl oxygen (HG) of Ser334 is 1.93 ± 0.48 Å. The hydrogen bond between the HE2 of His332 and the O7N of NAD$^+$ in the E·TS complex (average distance is 1.99 ± 0.19 Å) is shorter than that in the E·S complex (2.25 ± 0.35 Å). The average distance between the ND1 of His332 and the HE21 of Gln313 is virtually the same (2.07 ± 0.16 Å) as in the ground state. In both the E·S and E·TS complexes, bonding between His332 and Gln313 is of equal importance in maintaining the orientation of the His332 imidazole.

Additional changes were observed in conserved amino acid interactions upon going from the E·S to E·TS. The formate hydrogen (HF) in the TS structure is always directed away from the HE2 of His332, such that the average distance between these two atoms is 3.85 ± 0.30 Å. We previously considered the possibility of this interaction in the E·S complex (average distance 3.02 ± 0.71 Å) being involved in directing the hydrogen to be transferred as H$^-$ toward the C4N of NAD$^+$. As the TS structure is formed, this auxiliary function of the histidine imidazole is no longer necessary. The distance between the amide oxygen of Ile122 and the planar nitrogen of the NAD$^+$ ring decreases in the E·TS, as evidenced by the longer average distances between it and the hydrogen of the 2'-OH of the NAD$^+$ ribose (here 5.48 ± 0.67 Å). In a similar manner, the average distance between the 2'-oxygen and the N1N of the pyridine ring is lengthened slightly from 3.43 ± 0.22 (in the E·S) to 3.53 ± 0.11 Å (Figure 5). It was also observed that the average Pro97 HE3 to formate OF1 distances were shorter for the E·TS complex (Figure 11b) than the E·S complex (4.70 ± 0.59
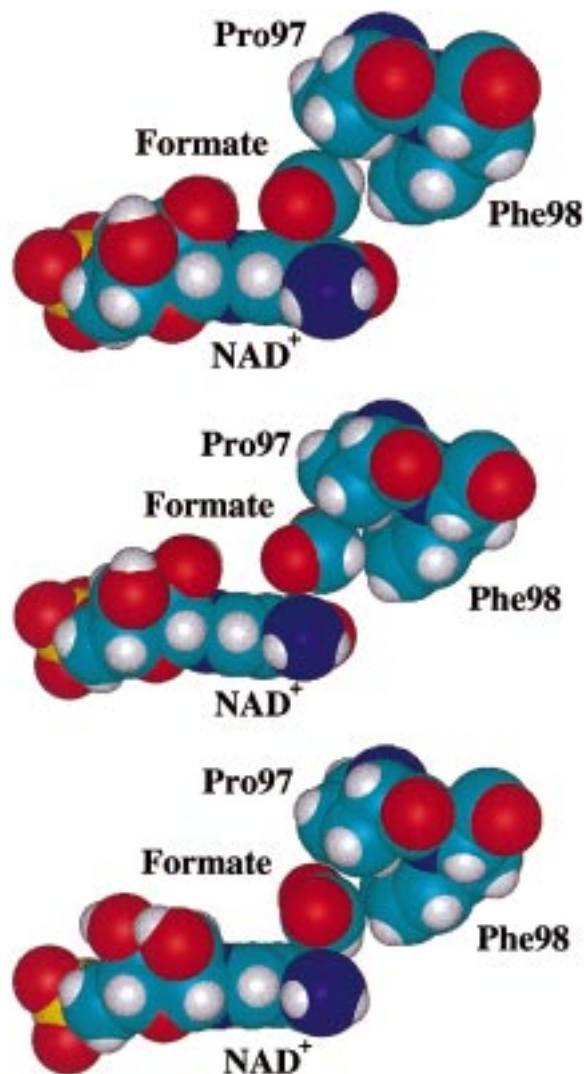

Figure 10. The steric bumping experienced throughout the MD simulation by the formate hydrogen during its oscillation about the binding pivot created by the electrostatic interaction of formate with Arg284, Asn146, and Ile122. The side chain of Phe98 provides a barrier to the motion of the formate hydrogen during its oscillation toward the C4N of NAD$^+$. Only the side chain of Phe98, formate, and the nicotinamide portion of NAD$^+$ are shown for clarity.

and 4.07 ± 0.71 Å, respectively). This is due, in part, to the charge and angle differences in the TS structure relative to the formate, which allow Pro97 and Phe98 to more closely approach the TS and facilitate the eventual product diffusion away from the catalytic site.

Differential Interactions between the E·S and E·TS Complexes. A comparison of bond lengths for the electrostatic interactions at the active site in the E·S, E·NAC (a subset of E·S consisting of only NAC structures), and E·TS complexes provides a clearer picture of catalysis by formate dehydrogenase. Results are presented in two tables. Table 1 allows comparison of the interaction distances between amino acid residues and formate in the E·S and the formate moiety of the transition state in the E·TS while Table 2 allows comparison of interaction distances with the nicotinamide moiety in the E·S and E·TS. One assumes that the shorter the observed distance of an electrostatic interaction, the stronger the interaction.

The interactions of Arg284 and His332 with the formate oxygen are significantly increased in the ground state compared to the transition state. The interactions between Asn146 and

(a)

(b)
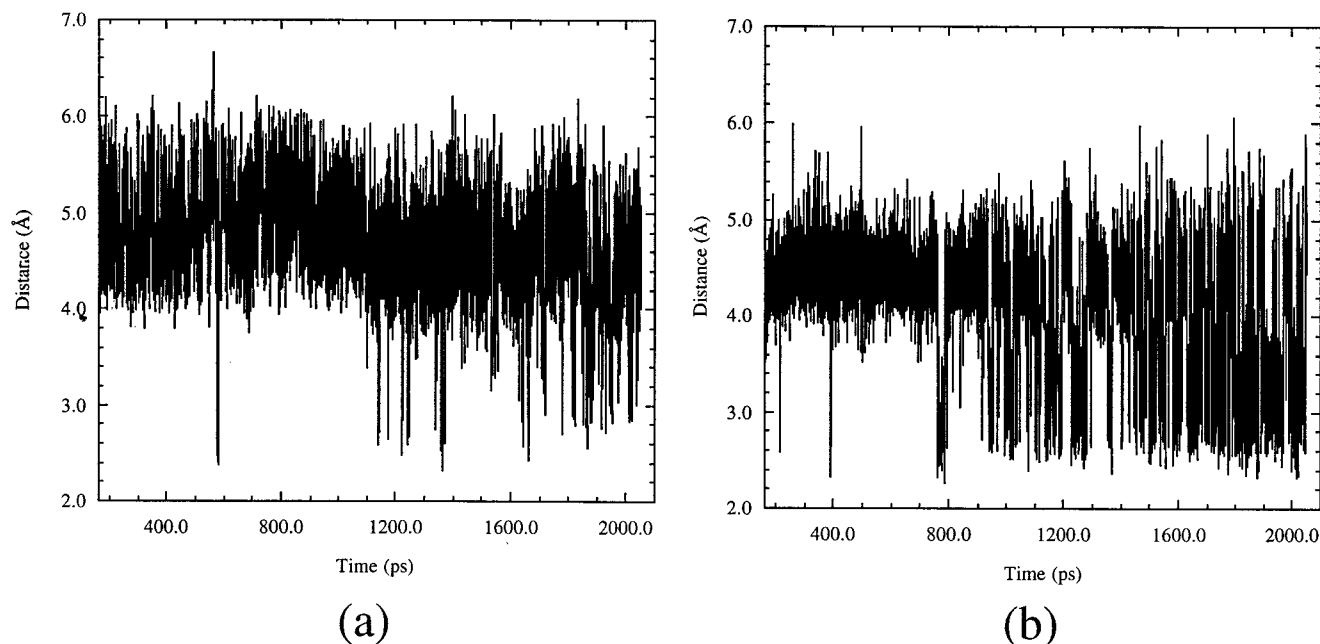
Figure 11. (a) Histogram of the distance between the HG3 of Pro97 and the O2 of formate in the E·S complex during the production dynamics. The shortest distances here correspond to NAC structures. (b) Histogram of the Pro97 HG3 to the transition state OF1 distance in the E·TS complex. Both Pro97 and Phe98 appear to act in concert to direct the formate hydrogen toward the C4N such that NACs form, thus assisting in hydride transfer.
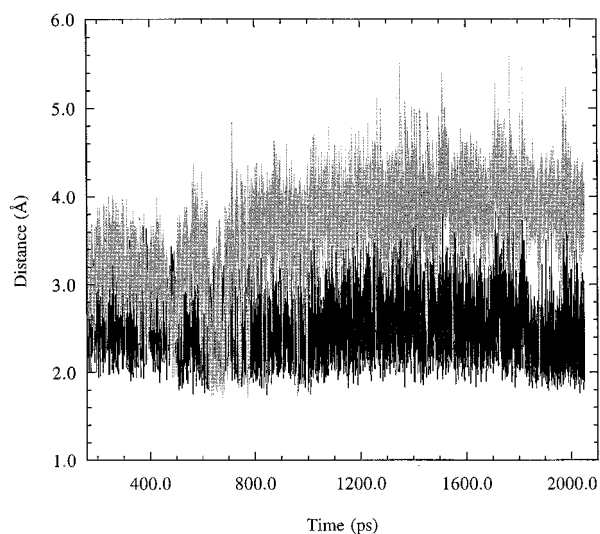
Figure 12. Plots of distance vs time for H72 of NAD$^+$ to Ser334 OG (black) and H72 to Asp308 OD1 (gray). Note the persistent hydrogen bond that is formed between Ser334 and the amide proton of NAD$^+$ relative to that of Asp308. This plot differs from that observed in the E·S complex in that these two amino acids do not appear to be working in conjunction with one another to maintain the *trans* conformation of the carboxamide arm.

Table 1. Average Interaction Distances (Å) between the E·S, E·NAC, and E·TS Complexes for the Formate Moiety

interaction	E·S	E·NAC	E·TS
Arg284 HH22−formate O1	1.98 ± 0.22	1.94 ± 0.15	2.32 ± 0.29
Arg284 HH12−formate O1	1.86 ± 0.13	1.87 ± 0.16	2.02 ± 0.18
Asn146 HD21−formate O2	1.88 ± 0.17	1.95 ± 0.19	1.94 ± 0.14
Ile122H−formate O2	1.98 ± 0.23	1.90 ± 0.12	2.05 ± 0.19
His332 HE2−formate O1	2.84 ± 0.40	2.71 ± 0.33	3.19 ± 0.45
His332 HE2−formate H1	3.07 ± 0.71	3.48 ± 0.38	3.85 ± 0.30

Ile122 with the other formate oxygen remain essentially the same in ground and transition states. These observations can

Table 2. Average Interaction Distances (Å) between the E·S, E·NAC, and E·TS Complexes for the Nicotinamide Moiety

| interaction	E·S	E·NAC	E·TS
His332 HE2−NAD$^+$ O7N	2.25 ± 0.35	2.49 ± 0.40	1.99 ± 0.19
Thr282 O−NAD$^+$ H71	1.87 ± 0.12	1.88 ± 0.12	1.88 ± 0.12
Asp308 OD1−NAD$^+$ H72	3.78 ± 0.58	2.82 ± 0.67	3.58 ± 0.56
Ser334 OG−NAD$^+$ H72	2.69 ± 0.40	2.64 ± 0.40	2.55 ± 0.35
Ser334 HG−Asp308 OD2	2.23 ± 0.57	2.18 ± 0.58	3.02 ± 0.74

be explained by the fact that the negative charge on the formate oxygens decreases upon going from the E·S to the E·TS (Scheme 4).

From Table 2, it can be seen that the hydrogen bonding interactions between the amide hydrogens of NAD$^+$ and Thr282 and Ser334 have not changed significantly between the ground state and transition state complexes. However, there is a significant change in the hydrogen bond distances between HE2 of His332 and O7N of NAD$^+$ between the E·S and the E·TS complexes. This hydrogen bond is shorter in the E·TS complex than either the E·S or the E·NAC. This is due to the increase in the partial negative charge on the amide carbonyl (O7N) on going from NAD$^+$ to the TS structure (Scheme 5). Taken together, the data in Tables 1 and 2 show a lengthening of the hydrogen bonds between Arg284 and formate in going from the E·S to the E·TS that is coupled with a shortening of the hydrogen bond between His332 and the carboxamide oxygen of NAD$^+$.

Conclusions

Our approach in the use of molecular dynamics simulations to compare enzyme·substrate and enzyme·transition state interactions, when the intrinsic enzymatic TS and calculated TS can be shown to be much the same, is novel. The judicious use of molecular dynamics simulations in this manner has allowed us to advance the structural knowledge associated with the hydride transfer reaction in formate dehydrogenase. The conserved amino acids Arg284, Asn146, and Ile122 serve to orient

Scheme 5

E·S   E·TS
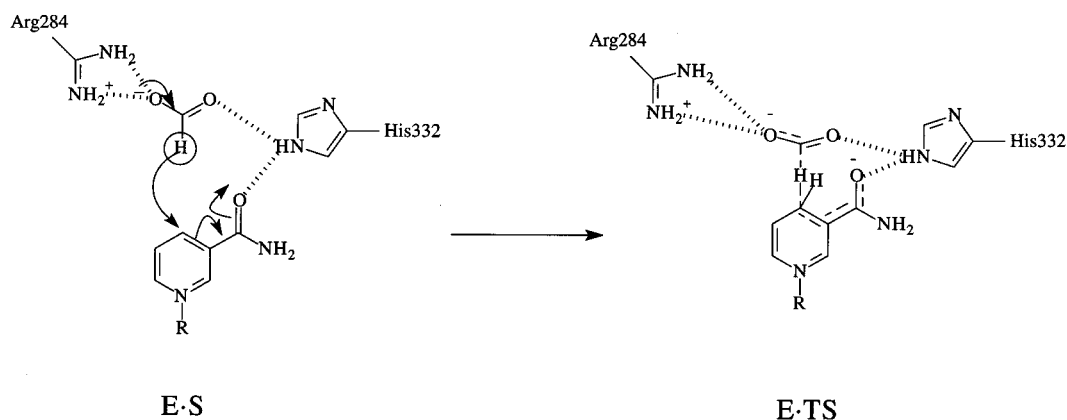
the formate substrate in the active site by electrostatic interactions with the formate carboxyl oxygens, resulting in a pivot about which the formate C–H moiety swings above the C4N of NAD⁺. The NAD⁺ oxidant has little motion. The carboxamide of NAD⁺ remains in the *trans* conformation throughout the MD simulation as a result of its interactions with the conserved amino acids Thr282, Asp308, His332, and Ser334. The HE2 of His332 participates in a tight hydrogen bond with the O7N of the carboxamide group. This hydrogen bond lengthens slightly when the HE2 of the histidine functions to direct the formate hydrogen toward the C4N (i.e. 30° attack angle). The HE2 of His332 also hydrogen bonds with formate O1 during NAC formation. These interactions of His332 with formate may be related, in part, to the lack of substrate binding in the H332F mutant.[48]

Upon going from the ground state to the transition state in the hydride transfer reaction, it is expected that the interaction between the guanidinium group of Arg284 and the oxygen (O1) of formate would decrease while the interaction of His332 with the amide carbonyl of NAD⁺ would increase, as represented in Scheme 5. This is reflected in our simulation and shows the discriminatory response of the enzyme to the ground state and the transition state structures. However, our simulation does not support preferential binding of the enzyme to the transition state over the ground state. The findings suggest that the conserved amino acids in the active site of FDH function more to orient the substrate and cofactor rather than stabilize the transition state structure.

Although Phe98 is apparently necessary to help close the substrate binding channel and exclude water from the active site,[2,3] it appears to interfere with the hydride transfer step due to unfavorable steric interactions with the formate hydrogen. The hydrogen to be transferred from formate to the nicotinamide cofactor must maneuver around the side chain of Phe98 while the formate oxygens remain electrostatically bound to Arg284, Asn146, and Ile122 (Figure 10). The kinetically unfavorable interactions of substrate with the Phe98 side chain explains the observation that the majority of the conformations in the simulation are not suitable for hydride transfer (Figure 4). We propose that steric bumping between the formate hydrogen and the Phe98 side chain represents a barrier to the hydride transfer reaction such that the reactive conformations of E·S amount to only a small fraction (1.5%) of the total conformations being NACs. As Phe98 and Pro97 are conserved in all known FDH sequences, one might conclude that exclusion of water from the catalytic site must be a more important objective than the absolute rate for H⁻ transfer. It would be interesting to see the effect of the rate of hydride transfer upon mutating the Phe98 to smaller hydrophobic residues.